Journal of Engineering Science and Technology
Vol. 1, No. 2 (2006) 99- 118


# THE INTERACTION OF LIQUID DROPS WITH A ROTATING GAS STREAM WITHIN A RAPIDLY REVOLVING ANNULAR ENCLOSURE

A. Aroussi

The Department of Engineering, University of Leicester, University Road, Leicester, LE1 7RH, UK
Email: aa285@Le.ac.uk

**Abstract**

The flow phenomena occurring around a rotating shaft are extremely complex and are a common feature in turbomachinery such as the bearing chambers of aero engines. As the liquid jet impinges onto the shaft, circumferential streams of lubricating liquid droplets centrifuge away from the rotor surface and impinge onto the inner circumference of the stationary case. A further break-up of drops occurred whilst rotating around the shaft before impacting on to the casing surface.

Non-intrusive laser techniques have been employed to aid the visualisation processes and the analysis of the flow phenomena occurring within the rotating annular enclosure. Results reveal that, the liquid flow conditions and the shaft rotation regimes, along with the aerodynamic movement of the air circulating around the shaft influence the dynamics of the droplets and consequently the lubrication processes within the bearing chambers.

Keywords: Laser Sheet Visualisation, Two-Phase Flows, Liquid Films, Droplet Dynamics.

## 1. Introduction

The performance and the structural integrity of an aero engine is maintained by the effective lubrication of the bearings situated within the bearing chamber. This is done

**Nomenclatures**

| | |
|---|---|
| *HP* | High pressure |
| *IP* | Intermediate pressure |
| *l/m* | Litre/minute |
| *LSV* | Laser sheet visualisation |
| *rpm* | Rotation per minute |
| *W* | Weber number |
| *Greek Symbols* | |
| $\theta$ | Jet impact angle |

through a thermal management process which involves the removal of frictional heat generated within the bearing chamber by the lubricating fluid. Additional cooling of the bearings is provided by the air circulating between the dual layers of the bearing housing. The dynamics of fluids within the intricate physical nature of bearing chambers coupled with extreme operational conditions are highly complex. Further complications are introduced through the interaction of liquids and gases that escape to and from the neighbouring areas of the chamber that disrupt the supply of the lubricating oil towards the bearings causing them to over-heat and sustain damage. Therefore, to avoid catastrophic events of engine failures, it is essential that effective lubrication of the bearings is maintained at all times.

The lubricating oil is supplied through a nozzle, which impinges onto a high speed-rotating shaft. The resulting flow regimes aid the lubrication and the heat transfer mechanisms within such systems. However, exposure to extreme conditions within the system influences these mechanisms. Windage effects (circumferential velocities of the movement of the surrounding air) generated by the rotation of the shafts influences the performance of the lubricating jets, the drop dynamics and the flow phenomena prevailing within the bearing cavities.

In this respect, a rig that simulates the principle function of the HP-IP bearing chamber at its most simplified level was developed to study the flow phenomena occurring around the rotating shaft. Investigations, in this case, extends the previous studies of Aroussi et al [1 and 2] with the aim to scrutinise the gas/liquid flow phenomena resulting from the interaction of the lubricating inlet jet as it impinges onto the rotating shaft when exposed to various parametric conditions e.g. shaft speeds and flow rates.

The phenomena of gas/liquid flows, resulting from the interaction of the lubricating jet and windage flow around the rotating shaft in the simple rig are extremely complex. The processes for understanding the nature of complex flows were strategically devised so that each flow feature that participated in generating the complex flows were identified, isolated and scrutinised through visualisation processes. The principle findings provide detailed explanations to the behaviour of drops within a system of rotating assemblies that are directly related to bearing chambers.

There is a lack of available literature in relation to the studies of complex flows in bearing chambers and other rapidly rotating systems. The flow pattern that fits the research scenario, in this case is described as “annular flow” as defined by Hewitt G.F [3], where liquid flows on the wall of the tube as a film and the gas flows in the centre. The film at the bottom of the tube is thicker than the film at the top owing to gravitational effects giving drainage around the periphery. Some of the liquid film is entrained as small droplets in the gas core. This type of flow occurs when the gas flows at high rates. Gas velocities also form the strongest parameter that has a profound affect upon drop sizes. As revealed by Azzopardi et al [4] and Jepson [5]. The increased effects of gas velocities reduced the sizes of the drops (inclusive of Sauter Mean Diameters). The effects of increased liquid mass flux increased the sizes of the drops. Butterworth D et al [6], examined the mechanisms of entrainment and deposition for maintaining the film around a horizontal tube and revealed that the rate of droplet entrainment is high in areas where the liquid film thickness is greatest and low in areas where the film tends to be thinner. The mechanisms involved as liquid drops impinge onto solid stationary surfaces have also been investigated by the authors. Wachters et al [7] studied the effects of liquid drops impacting onto a hot surface. Analysis from that investigation revealed that Weber (We) numbers could be used to describe the mechanisms involved with drop disintegration. When $We < 30$ no splash occurs, when $30 < We < 80$ the drop breaks after bouncing from a solid surface and when $We > 80$ splash also occurs. The critical conditions at which break-up occurs dependent upon the balance of inertial forces to surface tension forces of the liquid; namely the Weber number. A few preliminary studies by Wittig [9] and Wittig et al [10] emphasised that the oil droplet size is required in order to achieve a detailed analysis of the heat transfer mechanism inside the chamber. The first feasibility study of the oil droplet flow inside a bearing chamber was performed by Glahn et al [11] in which they conducted both the experimental and theoretical studies to obtain the required information of droplet sizes and their velocities. The research, in this case, aims to achieve a comprehensive understanding of flow effects occurring within complex systems with the aid of a suitably designed rig.

The visual interrogation of the gas/liquid flow processes around the rotating shaft are carried out using Laser Sheet Visualisation (LSV) to investigate the formation of liquid films and the flow patterns generated from the interaction of the lubricating jet with the windage gas stream. The effects of each feature are scrutinised for various parametric conditions.

## 2. Experimental Arrangement for Laser Sheet Visualisation (LSV)

The apparatus arrangement for LSV is shown in Fig. 1. The rig consists of 2 concentric cylinders. The inner shaft (60mm diameter, 600 mm in length) capable of rotating at speeds up to 5000 rpm and is enclosed by a stationary cylinder (140 mm internal diameter) made from clear Perspex to allow internal viewing. The continuous laser sheet is positioned in the central plane of the rig. The high-speed camera (Kodak motion analyser SR 3000) is positioned perpendicular to the laser sheet. The viewing orientations are varied according to each investigative stage. Water (simulating the lubricant fluid) is introduced through a simple nozzle (3mm diameter) placed centrally upon the upper surface of the Perspex stationary casing as a gravity driven jet stream. The shaft was set into motion and the results were recorded for various water flow rates ranging from 0.05 to 0.375 l/m and the shaft speeds varying from 0 to 5000 rpm.

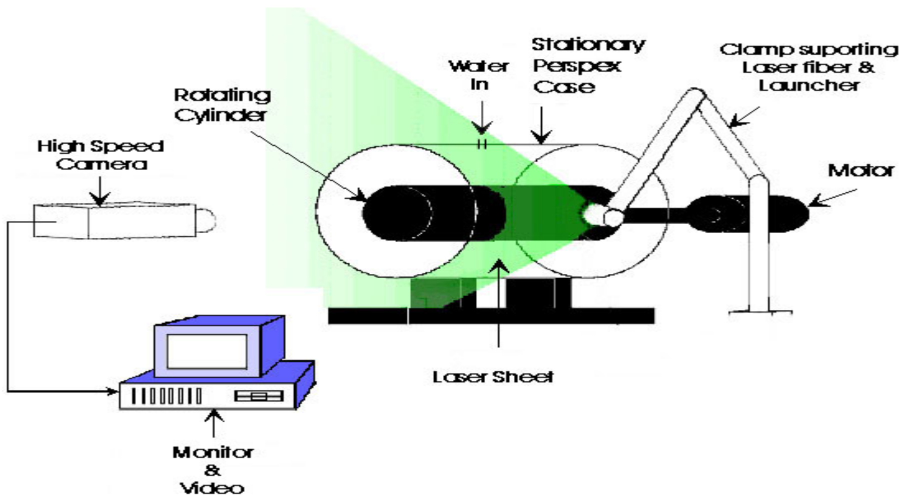


**Fig. 1. Laser sheet visualisation set-up.**

## 3. Results and Discussion

The phenomena two-phase gas/liquid flows resulting from the interaction of the lubricating jet and windage flow within the rotating annular enclosure were scrutinised. Observations were made in both planes of the rig (front and side) to monitor the action of each flow feature. The effects of each feature were scrutinised for various parametric conditions.

### 3.1. Gas/liquid flow patterns

Using the LSV apparatus shown in Fig. 1, the typical two-phase gas/liquid flow events show circumferential streams of water droplets centrifuging away from the surface of the rotating shaft and onto the internal circumference of the stationary case (Fig. 2). The main flow patterns originate in the following areas:

1. Rotating Shaft region
2. Stationary Case region
3. Air Phase region.

These regions govern the primary, secondary and tertiary flow regimes that influence the flow phenomena within the system.

**Fig.2. Flow patterns around a rotating annular system.**

The primary flow pattern evolves from the rotating shaft region. Streams of water droplets break off from the shaft film and are directed towards the stationary case (Fig. 3). The drops upon impact form a film on the internal surface of the stationary casing, which is preserved from the continuous impaction of the drops.

The secondary flow patterns occur near the casing region and are more complex due to different scenarios that influence the drop dynamics (Fig. 4). The path that the droplets take is dependent upon the direction of shaft rotation and the size of the droplets. The behaviour of larger drops is responsible for creating the complex flow patterns observed within the rig. The dynamics of drops changes with respect to increased rotor speeds as more drops of increasing sizes are forced to follow the flow of air and re-circulate around the shaft forming the tertiary flow pattern (Fig. 5). Other noticeable changes include the increase of entrainment and deposition rates, the reduction of droplets sizes and the increase of jet deflection angles that encourage the flow patterns to shift down stream in the direction of rotation.

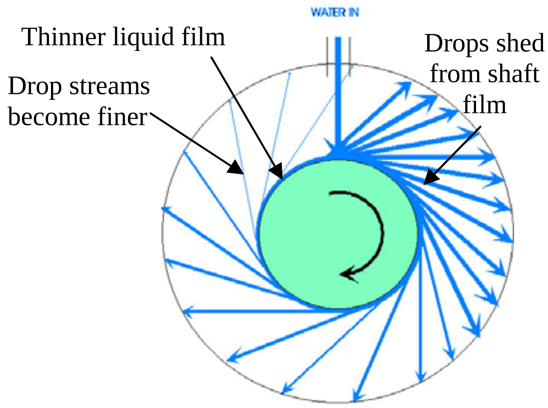


**Fig.3. Flow patterns from the shaft region.**

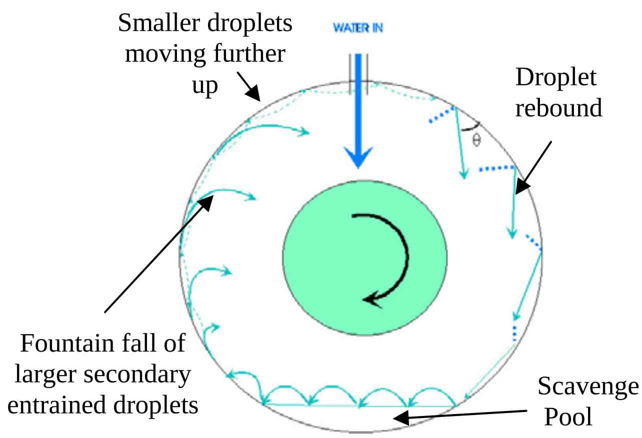


**Fig.4. Flow patterns from the stationary casing.**

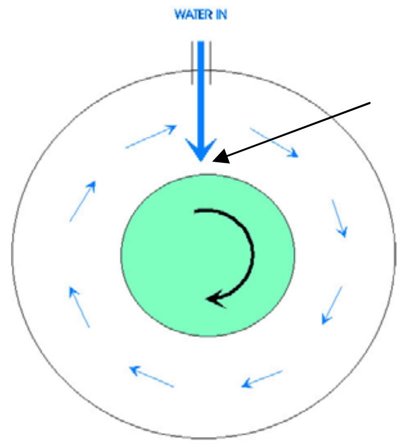


**Fig.5. Air flow patterns.**

The behaviour of drops is influenced by the operational conditions of the rig, the liquid inlet flow rates and the direction of the rotor motion. Each pattern interacts with the other and helps maintain the films within the annular enclosure.

## 3.2. Liquid film and droplet flow effects

Events such as, the formation and the behaviour of liquid films, the evolution of the drops from films and the formation of films through the interaction of drops were investigated using pigmented liquid in conjunction with digital photography. The shaft was covered with a grid to aid measurement and to provide reference points for further measurements. The liquid was injected in the central plane of the rig and onto the central point of the grid. Laser light was used to illuminate the interrogation areas and the camera was positioned perpendicular to the shaft and central to the liquid jet. Further visual illumination was provided using white light. The film effects on the shaft, the casing and the flow patterns encouraged by the interaction of the jet were observed for various parametric conditions and are summarised as follows:

### *3.2.1. Jet / film interaction*

The film effects differ for each corresponding parametric condition. For instance, in a stable environment (shaft in stationary condition), the inlet jet stream flows smoothly and falls around each side of the shaft forming a 'primary film' on the shaft surface. The film forms a band around the shaft surface with distinctive liquid build up areas (ligaments) at the borders (Fig. 6). The spread pattern of the liquid film on the shaft at each angular interval for various flow rates is presented in Fig. 7 and the variations of the film thickness across the 90° area of the shaft are displayed in Fig. 8. The film spread is widest in the jet impact area (0°) due to the continual feed of the fluid, and narrow in the 180° region of the rig due to the continual removal of the liquid. The back view of the rig produced symmetrical results to that of the frontal view plane. Further, the changes in colour tone of the liquid verify the variation of film thicknesses across the band. Darker areas, at the borders refer to areas of greater film thickness and the lighter area in the middle of the film band; show that the film is thin. Increasing the volumetric inlet flow rates increases the spread and the thickness of the film on the shaft surface.

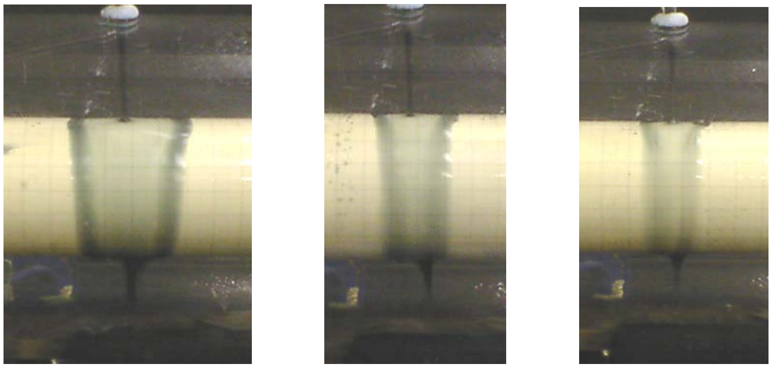

**0.375 l/m 0.2 l/m 0.05 l/m**

**Fig.6. Film spread and ligament effects on the stationary shaft.**

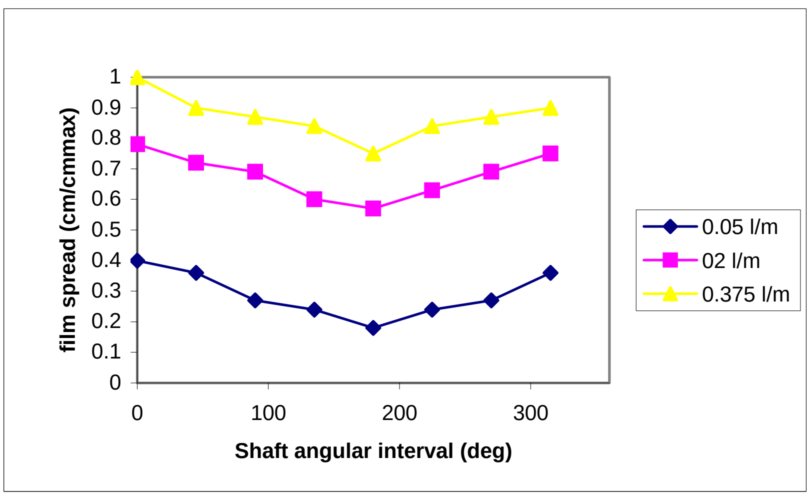


**Fig.7. Variation of film spread at each angular location on the stationary shaft.**

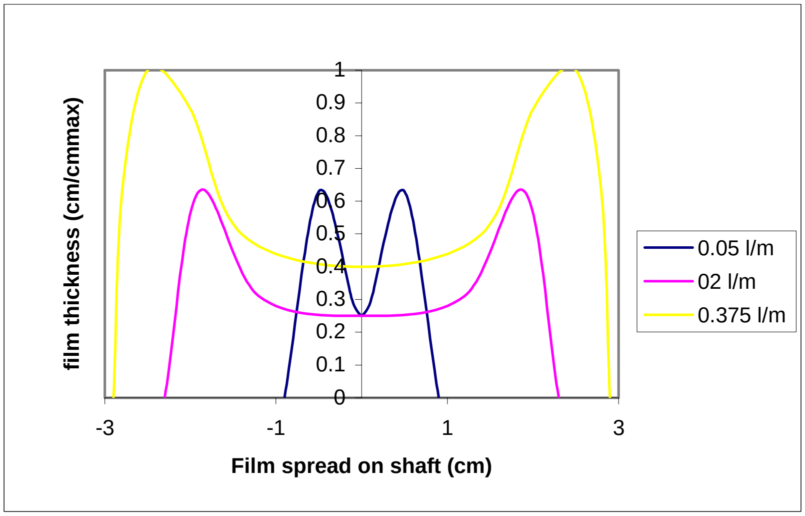


**Fig.8. Variation of film thickness across the film band at 90° location.**

As the shaft is set into motion, liquid from behind the shaft is pushed up in the direction of the rotor motion (Fig. 9) and eventually builds up behind and around the jet impingement area as a parabolic shaped ligament wrapped around the surface of the shaft (Fig. 10). Drops are shed tangentially both from the film ligament and the rotor surface and impinge on the inner surface of the perspex case. The overall spread of the film band on the shaft at each angular interval remained at a constant width around the shaft at each rotor speed interval (Fig. 11), but decreased in width with respect to increased rotor speeds (Fig. 12). The reduction of the film spread occurred through the increased effects of centrifugal forces that encouraged the removal of larger quantities of liquid from the film. Additionally, the rate of the liquid removal from the shaft film is also greater in comparison to the rate of the film formation on the shaft that is encouraged from the inlet jet.

The variations of the parabolic film spread on the shaft measured from the central plane of the jet for various shaft speeds are displayed in Fig. 13 and for various liquid flow rates are presented in Fig. 14. The characteristic shape of the ligament film remained the same irrespective of the varying conditions (Fig. 15). The profile of the parabolic curve narrowed in width and shifted downstream of the shaft relative to increased rotor speeds which as a consequence affected the flow characteristics observed within the rotating annular enclosure.

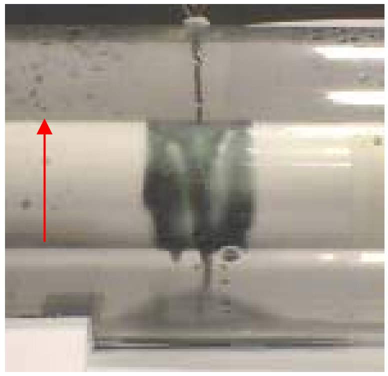

**Fig. 9. Film being pushed up from the rear of the shaft**

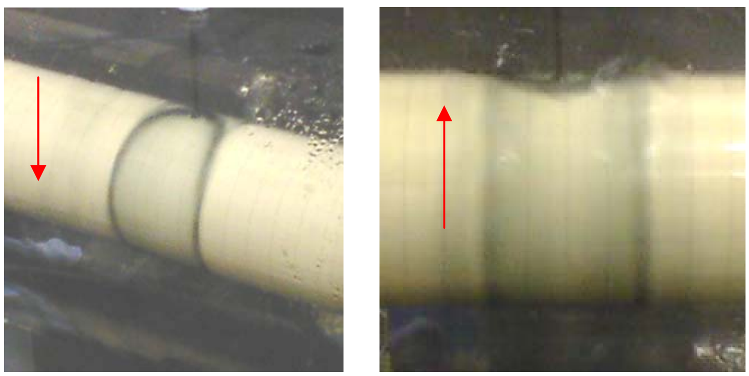

**Front view** **Rear view**

**Fig.10. Parabolic ligament film wrapped around the rotating shaft.**

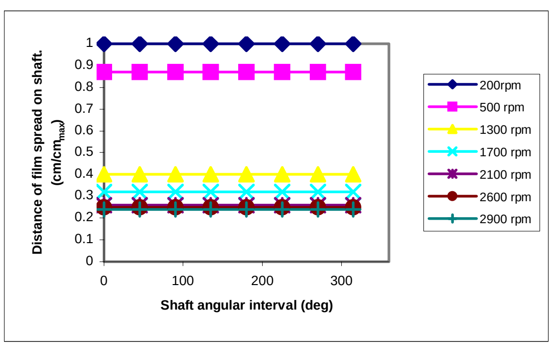


**Fig.11.Film spread effects at each angular location for 0.375 l/m for various rotor speeds**

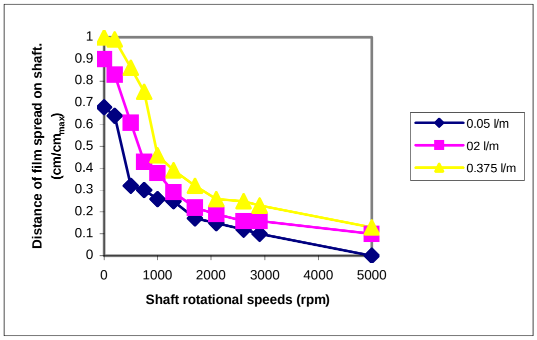


**Fig.12. Variation of (full) film spread for increase rotor speeds at 0°.**

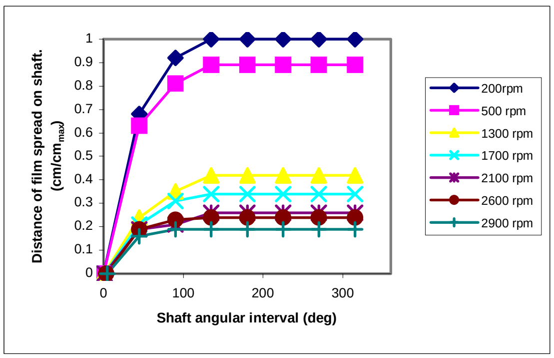


**Fig.13. Variation of parabolic cone for 0.375 l/m for various rotor speeds.**

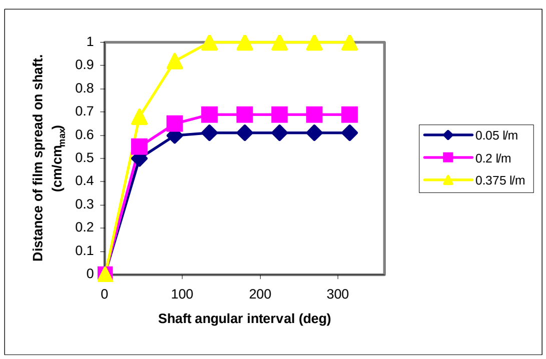


**Fig. 13. Variation of parabolic cone for 0.375 l/m for various rotor speeds.**

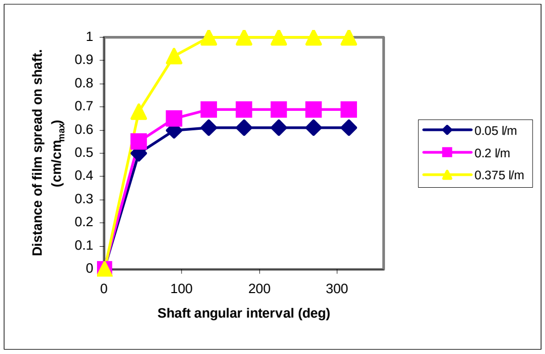


**Fig.14. Variation of parabolic effects at 200 rpm for various flow rates.**

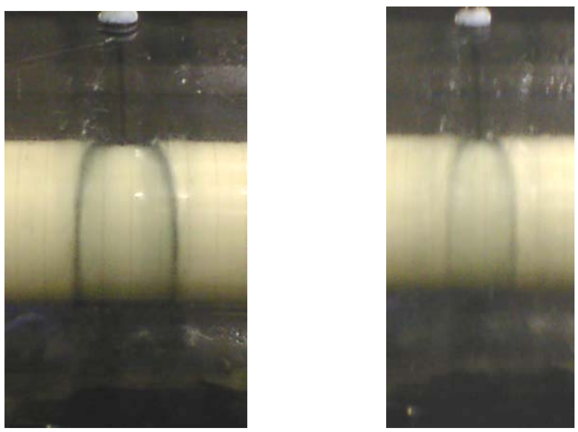

**200 rpm** **1300 rpm**

**Fig.15. The film spread effects on the shaft for various rotor speeds (0.375 l/m).**

### *3.2.2. Primary film/ primary drop interaction*

The process of drop shedding is also encouraged by centrifugal forces of the rotating shaft. The droplets are shed from the waves of the ligament film in the same manner as droplet entrainment. Drop entrainment from films occurs when the wave of the film reaches to a peak height and is torn away from the surface in the form of a drop. The tangential drop shedding patterns that occur from the parabolic ligament of film form of two streams either side of the jet impact area (Fig. 16). The drops are shed consecutively, one after the other forming a train. The profiles produced by the train of droplets form the patterns observed within the annular cavity of the rig (Fig. 17).

The impact positions of the droplets help determine the hot spot areas prevailing on the casing surface. Additionally, the limiting range of the droplet impact can also be determined. The scatter angles of the droplets shed from the parabolic arc of the ligament, in particular, the angle between the drops that impinges in the 90° region of the perspex casing was measured (Fig. 18) and the variation of the maximum scatter angle in relation to rotor speeds and liquid flow rate is presented in Fig. 19. Results highlight, that the scatter angles reach up to a peak value at 1300rpm (e.g., 96° for 0.2 l/m). As shaft speeds rise, greater quantities of liquid are lost from the shaft film reducing the spread and the parabolic arc of the ligament film. The jet also deviates further downstream of the shaft in the direction of rotation encouraging the scatter angle to shrink (e.g., 58° at 2900 rpm for 0.2 l/m). The results imply that hot spots are most likely to occur in the central plane of the jet stream and will eventually disappear as the dispersion of the scattered droplets is reduced. Further, the scatter angles of the droplets in excess of the depicted profiles will fall elsewhere on the shaft or in the scavenge pool.

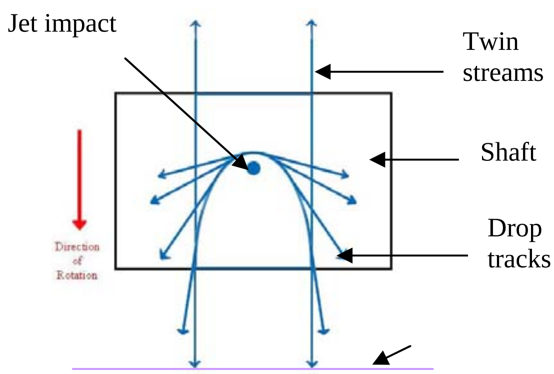


**Fig. 16. Drop shedding from ligament film from the rotating shaft.**

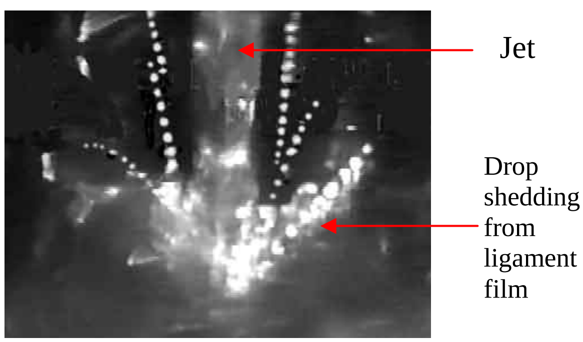


**Fig.17. Drop shedding effects from the ligament film behind the jet.**

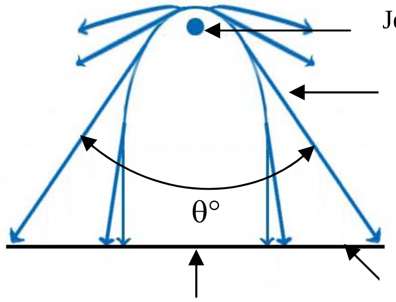


**Fig.18. Evaluation of scatter angles.**

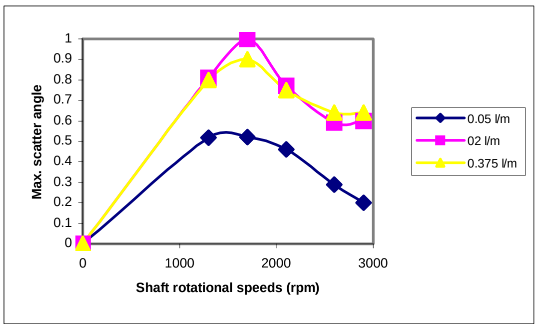


**Fig.19. Variation of scatter angles impinging on casing surface.**

### *3.2.3. Drop and secondary film interaction*

Drops shed from the rotating shaft, precipitate to form a 'rim' film on the inner surface of the Perspex case. The continual impaction of the droplets preserves the film on the casing surface. For each corresponding parametric condition (liquid inlet flow rates and shaft rotation speeds), the film spread on each side of the view plane of the rig of the casing surface differed as presented in Fig. 20.

Two streams of drops, shed tangentially from the shaft surface are deposited perpendicularly onto the Perspex case. Angular impact of the droplets occurs in the regions of the parabolic arc of the ligament film near the jet impact area creating a larger spread of film on the case located in the 90° region. The effects of increased rotor speeds has a narrowing effect upon the separation distances of the primary droplet streams, hence the deposition of these drops cause less dispersion of the casing film. The increased effect of liquid inlet flow rates increases the stream separation distances and hence increases the dispersion of liquid on the casing. Observations of the films on the casing showed that at high flow rates (0.375 l/m) and low rotor speeds (< 1300 rpm), the shaft drop shedding separation distance was too great to form a primary impact film in the central plane of the jet area. Large gaps of no film zones occur in the central plane of the inlet jet, thus revealing the hot spot zone prevailing on the casing surface. Hypothetically, if bearings where situated in the area, they would be subjected to a greater risk of damage.

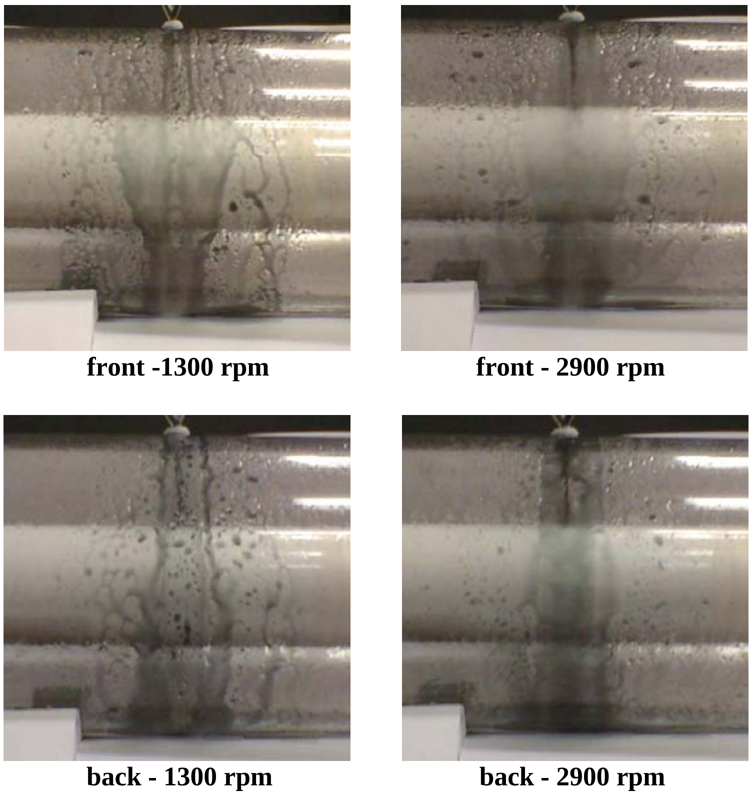


**Fig.20. Film on the surface of the Perspex casing for 0.375 l/m.**

### *3.2.4. Secondary film/secondary drop interaction*

As drops impinge onto the Perspex casing, the liquid is dispersed out until the gravity drags the film downwards. The spread of film is dependent upon the size of the droplet and equally, the Weber numbers. Higher Weber numbers prevail in conditions where the drop sizes are small. Small drop sizes usually prevail in conditions when the shaft rotational speeds are high. Smaller drops upon impact create a smaller spread of film on surfaces.

Secondary entrainment patterns are described in section 3.1. Secondary droplet entrainment occurs tangentially from the secondary ligaments, formed from droplet impact, and the casing curvature. The windage effects carry the entrained droplets in 2 ways; larger drops fountain down towards the shaft or the scavenge area; Smaller drops are re-deposited further up on the casing. The casing film areas can be mapped as primary impact and secondary impact zones. The spread of each zone is governed by rotor speeds. For instance, the primary film dispersion decreases whereas the secondary film dispersion increases in relation to increased rotor speeds (Fig. 21). The film thickness of each film zone also varies across the casing. For instance, the film in the primary impact zone is thicker in comparison to the secondary impact zone. These differences arise due to the different drop sizes that impinge in the casing surface. Droplets impacting in the primary zone are larger than those that impinge in the secondary film region. Film thicknesses at each angular cross-section also varied (Fig. 22). Droplet dispersal from the parabolic curvature of the shaft ligament film is wider, therefore creating a wider spread of liquid upon impact in the 90°area. Whereas, the film spread in the 270° cross-section is narrower due to the tangential impact of the primary droplets. The variation of the film thickness on the casing surface also reveals the ligaments from where the secondary droplets originate. The profile of the film thickness changes with respect to shaft rotation speeds and relative to the primary/secondary droplet impact zones. The reduction in the spread of the primary film encourages the film to thicken and further to form the secondary casing film. Altering the liquid inlet flow rates also affects the film thickness profiles across the casing surface. Figures 23 depict the reduction on the film thicknesses as the liquid flow rates are reduced.

The variations of film thickness across the casing surface hypothetically indicate the thermal variations on the casing. For instance, the secondary film zone will be hotter in comparison to the primary film zone.

Efficient component cooling is achieved by several governing factors eg, the continual precipitation of drops on the casing surfaces to form films. Gravitational and secondary entrainment ensures the film is constantly moving to aid fast and efficient heat exchange and to aid the preservation of the quality of the oil.

## 4. Conclusions

Complex flows, resulting from the interaction of the lubricating jet and windage flow, within rotating assemblies were broken into component features. The behavioural effects of each feature were scrutinised for various parametric conditions. The flow events prevailing within the gap between the rotating shaft and the stationary casing are summarised as follows:

1. Liquid films on surfaces are formed through the interaction the lubricating jet and droplet deposition. Droplet are shed /entrained from waves surfacing on the liquid films, and released tangentially from the ligament profile and the surface on which the film resides.
2. The sizes of the droplets, generated from films, are dependent upon the thickness of the liquid films. For example, drops of larger sizes are generated thicker films.
3. Droplet shedding/entrainment occurs from regions were films are of greater thicknesses and are deposited in areas where there is no or little liquid. For example, drops are released from the shaft film and are deposited onto the stationary casing. Further more, as the film on the shaft begins to diminish;

droplets entrained from the casing film are deposited on to the shaft. This way the flow phenomena occurring within the rotating systems are in a state of balance.

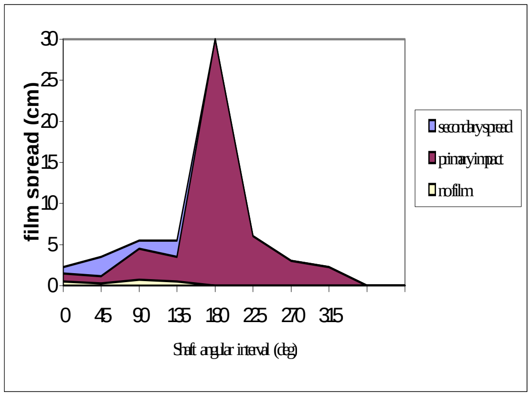


**1300 rpm**

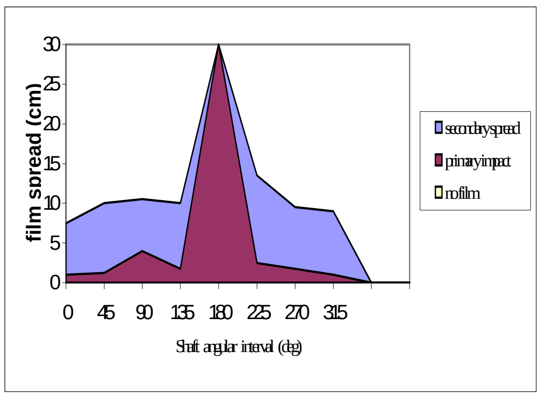


**2900 rpm**

**Fig.21. Variation of the film zones for 0.375 l/m.**

The flow phenomena within annular enclosures are significantly affected when exposed to parametric conditions. For example, increased rotor speeds generate greater aerodynamic forces that cause the lubricating jet to deviate. Equally, the rate of entrainment and deposition of droplets increases and the sizes of the entrained droplets become smaller. In overall, the behavioural patterns of the drops change as the system tries to maintain equilibrium of the flow occurring within it.

The increased effects of liquid flow rates encouraged further changes in the flow phenomena. The increased volumetric quantities of the liquid entering the rig encouraged the formation of thicker films. The changing effects of liquid films characterises the behaviour of drops, for example, sizes, trajectories, impact and rebound and break-up effects, which in turn influence the flow phenomena inside the system as a whole.

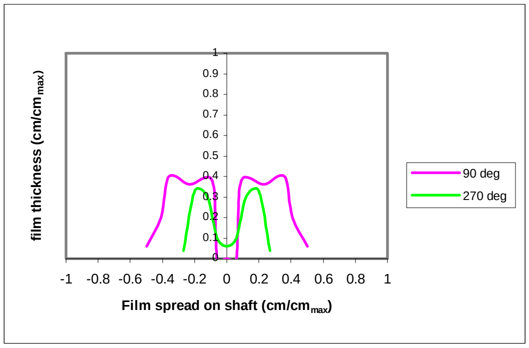


**1300 rpm**

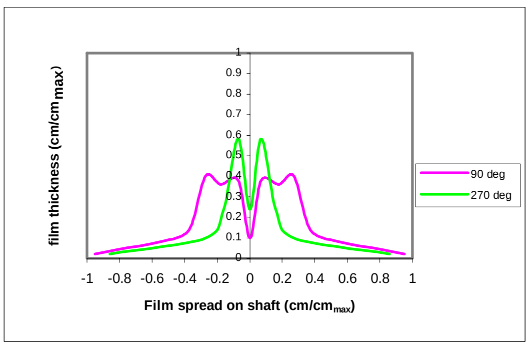


**2900 rpm**

**Fig.22. Variation of film thickness across the stationary casing for 0.375 l/m at 90 and 270 deg.**

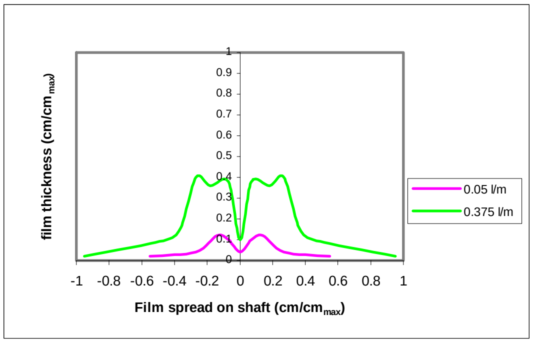


**90°**

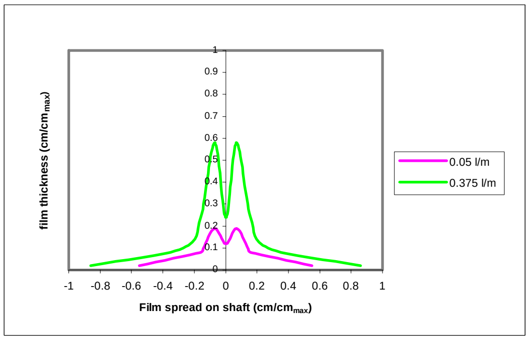


**270°**

**Fig.23. Variation of film thickness across the stationary casing for 2900 rpm various liquid flow rates.**

## References

1. Zaidi, S.H, Ishaq G., Aroussi, A. & Azzopardi, B.J (1998). Two-phase flow study around a rotating film using laser techniques. *Proceedings of Int. Conf. On Optical Techniques and Image Processing in Fluid, Thermal and Combustion Flow*, VSJ-SPIE, Yokohama, 6-10 December.
2. Ishaq, G., Aroussi, A., & Menacer, M. (2001). Flow visualisation of aerodynamic deflection effects on an inlet jet stream in an annular flow regime. *Proceedings of 3rd Pacific Symposium on Visualisation and Image Processing*, Paper F3481,8, Hawaii March.
3. Hewitt, G.F. (1978). Liquid mass transport in annular two- phase flows. *Proceedings of Int. Seminar momentum, Heat and Mass Transfer in Two–Phase Energy and Chemical Systems*, Dubrovnik.

4. Azzopardi, B.J, Freeman, G., & Whalley, P.B. (1978). Drop Sizes in Annular Two-Phase Flow. AERE-R 9074, Harwell.
5. Jepson, D.M. (1992). Vertical Annular Flow, the Effects of Physical Properties. PhD Thesis, University of Oxford.
6. Butterworth, D. & Robertson, J.M. (1977). Boiling and Flow in Horizontal Tubes. AERE, Harwell.
7. Wachters, H.J. & Westerling, N. A. J. (1963). The heat transfer from a hot wall to impinging water drops in a spherical state. *Chem. Eng. Sci*., 21, 1047- 1056.
8. Wittig, S. (1990). Heat transfer analysis in rotating gas turbine components: Experimental techniques and non-intrusive diagnostics. *Proceedings of The 3rd International symposium on Transport phenomena and Dynamics of rotating machinery*, Honolulu, USA.
9. Wittig, S., Glahn, A. & Himmelsbach (1993). Influence of high rotational speeds on heat transfer and oil film thickness in aero-engine bearing chambers, *ASME paper dsNo 93-GT-209.*
10. Glahn, A., Kurreck, M., Willman, M. & Wittig, S. (1995). Feasibility study on oil droplet flow investigations inside aero engine bearing chambers - PDPA techniques in combination with numerical approaches, *ASME paper No 95-GT-100.*